Circulation Research

ORIGINAL RESEARCH

Molecular and Spatial Signatures of Mouse Embryonic Endothelial Cells at Single-Cell Resolution

Jian Chen,* Xiaoran Zhang,* Daniel M. DeLaughter, Michael A. Trembley, Shaila Saifee, Feng Xiao, Jiehui Chen, Pingzhu Zhou, Christine E. Seidman, Jonathan G. Seidman, William T. Pu

BACKGROUND: Mature endothelial cells (ECs) are heterogeneous, with subtypes defined by tissue origin and position within the vascular bed (ie, artery, capillary, vein, and lymphatic). How this heterogeneity is established during the development of the vascular system, especially arteriovenous specification of ECs, remains incompletely characterized.

METHODS: We used droplet-based single-cell RNA sequencing and multiplexed error-robust fluorescence in situ hybridization to define EC and EC progenitor subtypes from E9.5, E12.5, and E15.5 mouse embryos. We used trajectory inference to analyze the specification of arterial ECs (aECs) and venous ECs (vECs) from EC progenitors. Network analysis identified candidate transcriptional regulators of arteriovenous differentiation, which we tested by CRISPR (clustered regularly interspaced short palindromic repeats) loss of function in human-induced pluripotent stem cells undergoing directed differentiation to aECs or vECs (human-induced pluripotent stem cell-aECs or human-induced pluripotent stem cell-vECs).

RESULTS: From the single-cell transcriptomes of 7682 E9.5 to E15.5 ECs, we identified 19 EC subtypes, including *Etv2*$^{+}$*Bnip3*$^{+}$ EC progenitors. Spatial transcriptomic analysis of 15 448 ECs provided orthogonal validation of these EC subtypes and established their spatial distribution. Most embryonic ECs were grouped by their vascular-bed types, while ECs from the brain, heart, liver, and lung were grouped by their tissue origins. Arterial (*Eln*, *Dkk2*, *Vegfc*, and *Egfl8*), venous (*Fam174b* and *Clec14a*), and capillary (*Kcne3*) marker genes were identified. Compared with aECs, embryonic vECs and capillary ECs shared fewer markers than their adult counterparts. Early capillary ECs with venous characteristics functioned as a branch point for differentiation of aEC and vEC lineages.

CONCLUSIONS: Our results provide a spatiotemporal map of embryonic EC heterogeneity at single-cell resolution and demonstrate that the diversity of ECs in the embryo arises from both tissue origin and vascular-bed position. Developing aECs and vECs share common venous-featured capillary precursors and are regulated by distinct transcriptional regulatory networks.

GRAPHIC ABSTRACT: A graphic abstract is available for this article.

Key Words: cell cycle ■ embryonic development ■ endothelial cells ■ single-cell gene expression analysis ■ transcription factors

In This Issue, see p 475 | Editorial, see p 547

Endothelial cells (ECs) are major components of the vascular system, directing its development, form, function, and homeostasis. During early vascular development, ECs acquire arterial, venous, capillary, and lymphatic identities.[1,2] Vascular development is integrated with organ specification and morphogenesis, and ECs specialize in an organotypic manner.[3–5] These parameters, vascular-bed position, and tissue origin are major components of EC heterogeneity. Adult EC heterogeneity is mainly determined by tissue origin.[3] The developmental timeline by which ECs establish their diverse, mature expression patterns is poorly defined. Current embryonic EC single-cell RNA sequencing (scRNA-seq) data[6,7] are limited to early developmental stages and do not

Correspondence to: William T. Pu, MD, Department of Cardiology, Boston Children's Hospital, 300 Longwood Ave, Boston, MA 02115. Email william.pu@cardio.chboston.org
*J. Chen and X. Zhang contributed equally.
Supplemental Material is available at https://www.ahajournals.org/doi/suppl/10.1161/CIRCRESAHA.123.323956.
For Sources of Funding and Disclosures, see page 544.

Circulation Research is available at www.ahajournals.org/journal/res

Novelty and Significance

What Is Known?

- Endothelial cell (EC) heterogeneity arises from their tissue source and vessel type, with tissue source being the main driver of heterogeneity in adult mice.
- Arterial ECs and venous ECs are specified early in embryogenesis although the steps and regulation of arteriovenous differentiation remain incompletely defined.

What New Information Does This Article Contribute?

- A first spatiotemporal single-cell map of embryonic ECs from E9.5 to E15.5.
- Tissue origin predominates the heterogeneity of embryonic brain, heart, liver, and lung ECs, while vessel bed origin predominates the transcriptional signature of other ECs.
- Newly identified markers of embryonic EC subtypes and transcriptional regulators of arteriovenous specification.
- Arterial ECs and venous ECs share a common intermediate plexus state, and arterial ECs form via arterialization of venous-featured capillary ECs.

We constructed a single-cell map of embryonic ECs that expand the developmental range beyond prior single-cell studies of vascular development. Through spatial transcriptomics, we mapped the distribution of embryonic EC subtypes. We show that tissue-specific signatures are established early in the development of the embryonic brain, heart, liver, and lung. In contrast, vessel bed type dominates the transcriptional signature of most embryonic ECs. We defined new molecular markers of several subtypes of embryonic ECs, including capillaries, veins, and tissue-specific ECs. Our analysis of arteriovenous differentiation trajectories suggests that most arterial ECs and venous ECs share a common intermediate precursor plexus state and that arterial ECs form by arterialization of venous features capillary ECs. Our spatiotemporal atlas will facilitate the study of vascular development.

Nonstandard Abbreviations and Acronyms

aEC	arterial endothelial cell
cEC	capillary endothelial cell
EC	endothelial cell
hiPSC	human-induced pluripotent stem cell
MERFISH	multiplexed error-robust fluorescence in situ hybridization
scRNA-seq	single-cell RNA sequencing
SMC	smooth muscle cell
TF	transcription factor
vEC	venous endothelial cell
vSMC	vascular smooth muscle cell

systematically clarify the origins of embryonic EC heterogeneity. Furthermore, current data lack spatial information.

The arteriovenous specification is a key step of early vascular development that contributes to EC heterogeneity by producing arterial ECs (aECs) and venous ECs (vECs). These EC subtypes have distinct molecular signatures and functions, but the steps by which aECs and vECs are specified remain uncertain. In classical models, they develop from different EC progenitors that are specified at different positions in early embryos.[8,9] An alternative model is that in certain tissues, aECs develop from vECs.[10–13] Recent scRNA-seq data were interpreted to support the embryonic conversion of vECs to aECs.[7,14]

The regulatory mechanisms governing arteriovenous specification have been intensely investigated. VEGF (vascular growth factor), Notch, and BMP (bone morphogenetic protein) signaling pathways regulate the differentiation of aECs and vECs during embryogenesis.[2,15–17] Additionally, the cell cycle is intricately linked to arteriovenous specification.[18,19] Arteriovenous specification is transcriptionally regulated, with transcription factors (TFs) *Sox17* and *Foxc1/c2* promoting aEC and *Nr2f2* (also known as COUP-TFII) promoting vEC differentiation.[20–22] However, the transcriptional mechanisms that mediate arteriovenous specification remain incompletely defined.

Here, we analyzed EC heterogeneity in murine embryos at key stages of vascular development (E9.5, E12.5, and E15.5). We present a comprehensive spatiotemporal single-EC transcriptomic map and identify the predominant determinants of embryonic EC heterogeneity. Furthermore, we provide a revised developmental tree for arteriovenous specification. We analyzed the transcriptional regulation of arteriovenous differentiation and identified USF1 (upstream transcription factor 1) as a novel TF that promotes aEC differentiation.

METHODS

Data Availability

Detailed methods are in the Supplemental Material. All material, data, and detailed protocols are available upon reasonable request. Please see the Major Resources Table in the Supplemental Material (Table S1). Animal experiments adhered

to protocols approved by the Boston Children's Hospital Animal Care and Use Committee. The data have been deposited to Gene Expression Omnibus (GEO): multiplexed error-robust fluorescence in situ hybridization (MERFISH): GSE247450; bulk RNA-seq: GSE247449; and scRNA-seq: GSE216970. Raw MERFISH data are available at https://zenodo.org/records/10655724.

RESULTS

Identification of Distinct EC Clusters in Mid-to-Late Gestation Mouse Embryos

We dissociated single cells from E9.5, E12.5, and E15.5 mouse embryos (Figure S1A). We used a modestly selective Magnetic-Activated Cell Sorting protocol for PECAM1 that maximized cell viability, enriched ECs, and included EC precursors (Figure 1A; Figure S1B through S1D). We then used microdroplet technology to capture and sequence 35 268 high-quality cells, including ECs, EC precursors, and other cell types. Following bioinformatic correction, minimal batch effects were evident (Figure 1E and 1F; Table S2).

Initial clustering identified ECs and 11 other cell types (Figure S2). We selected ECs based on the expression of *Pecam1*, *Cdh5*, or *Kdr*. These ECs included EC progenitors, which expressed *Kdr*, *Etv2*,[23,24] and *Bnip3*,[7] and had low levels of *Cdh5* and *Pecam1* (Figure 1B). EC clustering identified 20 subclusters with distinct marker genes

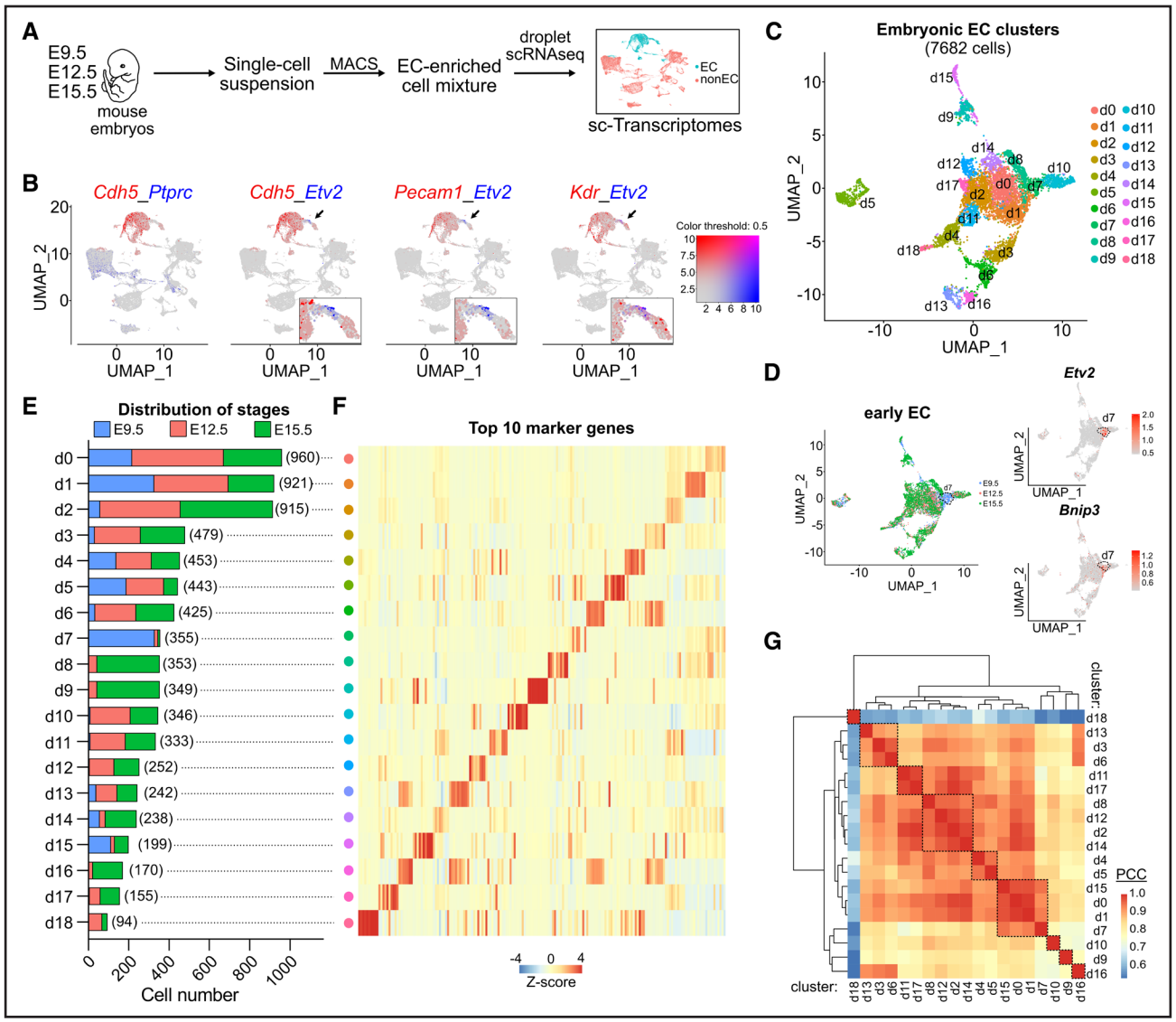

Figure 1. Single-cell RNA-seq profiling of endothelial cells (ECs) in mid-to-late gestation mouse embryos.
A, Scheme of single-cell RNA sequencing (scRNA-seq) experiment design. **B**, Feature plots of ECs and *Etv2*+ early ECs. Arrows indicate regions enlarged in insets, showing partial coexpression of *Etv2* and *Kdr*. *Ptprc* (CD45) labels blood cells. **C**, Uniform manifold approximation and projection (UMAP) plot showing 19 clusters of embryonic ECs. **D**, UMAP plots denoting *Etv2*+ early EC cluster. **E**, Bar plot showing the proportion of time points within each EC cluster. The bracketed number denotes the number of cells in each cluster. **F**, Heatmap of top 10 marker genes for each cluster. **G**, Hierarchical clustering and the Pearson correlation coefficient (PCC) heatmap of all EC clusters. The analysis was based on the signature enriched genes of each cluster identified by the Seurat FindAllMarkers function.

(Figure S3A through S3C). We excluded one distantly related cluster that likely represented EC-erythrocyte doublets that had escaped the doublet filter (Figure S3D and S3E).

The remaining 7682 ECs and EC precursors were grouped into 19 distinct droplet clusters (clusters d0–d18; Figure 1C). d7 cells, which express the EC progenitor markers *Etv2* and *Bnip3*, were mostly from E9.5 embryos, whereas d8, d9, and d16 cells were mostly from E15.5 embryos (Figure 1D and 1E). The EC subtypes had distinct gene expression signatures (Figure 1F; Figure S4; Tables S3i and S4i). Hierarchical clustering of the 19 EC subtypes identified 9 groups of most similar EC subtypes (dotted boxes, Figure 1G; Table S3ii). For instance, d7 early ECs were most similar to d0, d1, and d15 ECs.

Tissue-Specific Embryonic ECs

Prior scRNA-seq of adult ECs[3] demonstrated that their transcriptional signatures reflect tissue origin more than vessel type (Figure S5A). After we integrated these data with our embryonic EC data, only a small subset of embryonic ECs clustered with adult ECs (Figure 2A).

We used 3 separate approaches to leverage adult tissue-specific EC data to identify tissue-specific embryonic ECs. First, we predicted the tissue origin of embryonic ECs by transcriptome similarity to adult ECs (Figure 2B). A minority of embryonic ECs had high prediction scores: embryonic ECs from d3, d6, and d16 were similar to adult brain ECs, d5 to adult heart ECs, and d9 and d15 to adult liver ECs. The remaining embryonic EC clusters had low prediction scores or resembled mixtures from multiple tissues.

Second, from the adult EC data, we identified highly tissue-specific markers (Figure S5B) and used them to classify embryonic EC single-cell transcriptomes. Most embryonic ECs, including d7 (early ECs), did not express these adult tissue-selective EC markers in clear patterns, except for EC subsets that expressed brain, heart, or liver EC markers (Figure S5C). The prediction approach suggested that d9 resembled adult liver ECs (Figure 2B), but this inference was not supported by the marker analysis (Figure S5C).

Third, we experimentally measured marker gene expression in ECs isolated from individual tissues (brain, heart, lung, liver, kidney, and small intestine) dissected from tamoxifen-treated E12.5, E15.5, or adult Cdh5-CreERT2;Rosa26^{TdTomato} mice. We purified ECs from each tissue by flow cytometry (Figure S6A) and verified their purity by quantitative reverse transcription PCR (RT-qPCR; Figure S6B). Across this panel of individual tissue ECs, we measured 25 markers with selective expression based on the adult data. In adult ECs, 16 markers were validated as tissue-specific (Figure S6C). At E15.5, only 8 remained tissue-specific, and 3 additional markers were more specific at E15.5 than in adults (Figure S6D). A minority of adult tissue-specific EC markers were conserved across embryonic stages.

Collectively, these analyses supported the assignment of a subset of embryonic EC clusters to specific tissues: brain: d3, d6, and d16; heart, d5; liver, d15; and lung, d8. ECs from other tissues intermingled, indicating that their transcriptional signatures are primarily determined by other parameters. Additionally, these results indicate that tissue-specific EC markers change dynamically during development. This was further evident when the adult and embryonic EC data sets were examined for tissue-specific EC markers with dynamic developmental expression (Figure S6E). Embryonic brain, heart, liver, and lung selective EC markers with differential expression between stages included *Lrp8*, *Slc38a5*, *Hand2*, *Stab2*, and *Scn7a*, respectively.

Embryonic EC Vascular-Bed Heterogeneity

We next studied the contribution of vascular-bed type to embryonic EC heterogeneity. Recent scRNA-seq studies on adult ECs provided sets of vessel-type markers conserved among tissues.[3] These genes, combined with canonical vessel-type markers, were used to define the vessel types of embryonic EC clusters (Figure 2C and 2D; Figure S7A). The early EC cluster (d7) did not robustly express vessel-type markers, consistent with its precursor identity (Figure 2C). Clusters d4 and d18 expressed the highest level of nearly all arterial markers and high levels of large vessel markers (*Vwf* and *Vcam1*),[3,25,26] indicating that they were large artery ECs (artery_1 and artery_2). Cluster d12 showed the highest level of most venous markers in addition to large vessel markers *Vwf* and *Vcam1*, indicating that it contained larger vein ECs (vein). Clusters d0, d1, d2, d8, d11, d14, and d17 expressed varying subsets of capillary markers. Clusters d0 and d1 largely arose from earlier stage embryos (Figure 1E) and were most closely related to the EC progenitor cluster (d7; Figure 1G) and, therefore, were labeled as capillary plexus (plexus). The other capillary subsets arose predominantly from later-stage embryos and were labeled as capillaries (capil). Cells in d11 expressed arterial and capillary markers, suggesting an intermediate identity, leading to their designation as arteriole ECs (capil-a). Analogously, cells in d2 expressed both venous and capillary markers, leading us to label them as venule ECs (capil-v). Cells in d10 highly expressed lymphatic markers.

Embryonic EC clusters with tissue-specific markers variably expressed vascular-bed markers (Figure 2C). Brain ECs (d3, d6, and d16) highly expressed both brain and capillary EC (cEC) markers, with d3 and d6 also expressing arterial or venous markers, respectively (d3,

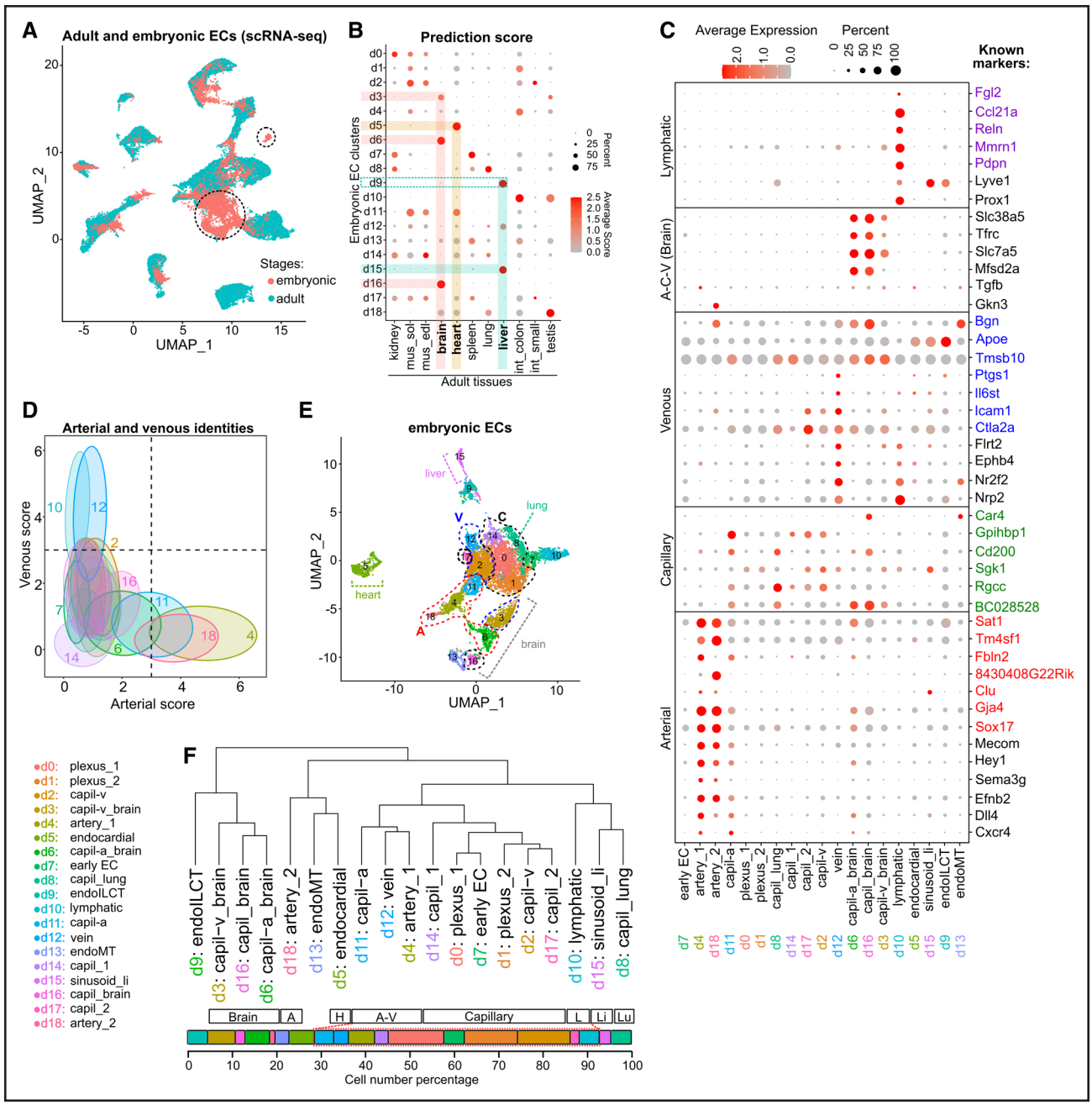

Figure 2. Heterogeneity of embryonic endothelial cells (ECs).

A, Integrative uniform manifold approximation and projection (UMAP) plot of ECs from adult (data set E-MTAB-8077 from reference [3]) and embryonic stages. **B**, Embryonic EC clusters scored for tissue-specific signatures of adult ECs. Shading indicates that the denoted cluster has a tissue-specific signature. **C**, Expression of known vascular-bed type markers in embryonic EC subtypes. The colored genes are adult markers conserved among tissues identified in reference [3]. **D**, Average arteriovenous scores of the cells in each cluster. Ovals denote the distribution ranges of arteriovenous scores in each cluster. Dashed lines indicate threshold values. **E**, Embryonic EC clusters annotated for identified expression signatures. **F**, Hierarchical clustering of all embryonic EC subtypes using variable genes across the data set. The bottom bar plot shows the cell number percentage of each cluster and the color indicating the cluster identity. A indicates arterial; capil-a, capillary arterial EC; capil-v, capillary venous EC; endoICLT, endothelial-to-immune-like cell transition; endoMT, endothelial-to-mesenchymal transition; H, heart; K, kidney; L, lymphatic; Li, liver; Lu, lung; sinusoid_li, liver sinusoid ECs; and V, venous.

capil-v_brain; d6, capil-a_brain; and d16, capil-brain). Lung ECs (d8) expressed cEC markers (capil-lung). Heart (d5) and liver (d15, sinusoid) ECs were poorly annotated by vessel-type markers. Heart ECs comprise endocardial ECs, which line the heart chambers, and vascular ECs, which line the coronary vessels. Cluster d5 highly expressed endocardial EC markers (eg, *Npr3*) but not coronary EC markers *Fabp4* and *Cd36*, indicating that d5 contains more endocardial ECs (Figure S7B). Liver ECs expressed sinusoid markers, such as *Stab2* and *Lyve1*

(Figures S6E and S7C). Two clusters, d9 and d13, did not show a clear pattern of tissue-specific or vessel-type markers. Based on the differentially expressed genes in these clusters, we annotated them as endothelial-to-immune-like cell transition[27] and endothelial-to-mesenchymal transition (Figure S7C through S7E; Table S5i).

To further characterize the vascular-bed type of each cluster, we scored the arteriovenous characteristics of all embryonic ECs using known arterial and venous marker genes (see Methods; Figure 2D). Clusters with arterial features (d4, d6, d11, and d18), especially the 2 large artery clusters (d4 and d18), had high arterial scores (Figure 2D). Large vein (d12) and lymphatic (d10) ECs showed similarly high venous scores (Figure 2D), in line with the origin of most lymphatic ECs from vECs.[28,29] Most cECs showed more similarity with vECs than aECs. This analysis further supports the annotation of clusters by vessel bed type.

Grouping of embryonic EC subtypes based on highly variable genes showed that vessel-type ECs clustered apart from the brain, heart, lung, and liver ECs and lymphatic ECs (Figure 2F) and comprised 70% of all ECs. Collectively, multiple analytical approaches show that transcriptomes of embryonic ECs from brain, heart, liver, and lung EC are distinguished mainly by tissue-specific signatures, while those of ECs from other sites are grouped by their vascular-bed position.

Spatial Distribution of Embryonic ECs

To verify the EC subtypes identified by scRNA-seq and map their spatial distribution, we performed MERFISH[30] experiments on sagittal sections obtained from E9.5 and E15.5 embryos (Figure 3A). We designed a 300-gene panel comprising classical EC and smooth muscle cell (SMC) markers and the top markers for each EC subtype identified by scRNA-seq (Figure 3B). All 3 samples showed high data quality, and 295 genes were successfully decoded and passed quality control (Figure S8A through S8F). EC and SMC markers were expressed in expected patterns, confirming the good quality of the MERFISH data (Figure S9A and S9B). We integrated all cells and selected ECs and SMCs based on scores calculated from known markers (15 448 ECs: *Etv2*, *Kdr*, *Cdh5*, and *Pecam1*; 5134 SMCs: *Myh11*, and *Acta2*; Figure S9C through S9I). These ECs were grouped by gene expression into 25 clusters (p0–p24) with distinct spatial distributions (Figure 3C through 3E). The majority of cells in each cluster originated from E15.5, except for the early EC cluster (p20), marked by *Etv2* and found mostly at E9.5 (Figure 3F).

To interrelate MERFISH and scRNA-seq data, we coembedded ECs from both data sets.[31] ECs from scRNA-seq and MERFISH intermingled well (Figure 4A; Figure S10A). MERFISH clusters p2, p4, p6, p9, p19, and p24 did not have scRNA-seq counterparts. We used 2 approaches to annotate the MERFISH ECs. First, we used the scRNA-seq ECs as a reference to predict the identity of each MERFISH EC and then scored MERFISH clusters by the fraction of cells with the highest prediction score for each scRNA-seq EC subtype (Figure 4B; Figure S10B). For example, most p0 ECs scored highest for d2 (capil-v); most p1 ECs scored highest for d1 (plexus_2). Other such mappings were p4 and p12, d6 (capil-a brain); p5, d5 (endocardial); p7, d4 (artery_1); p10, d10 (lymphatic); and p18, d9 (endothelial-to-immune-like cell transition; Figure 4B; Figure S9). Second, for each MERFISH cluster, we calculated the score of each scRNA-seq subtype's marker panel. These methods had excellent overall agreement, except for p20, which most highly expressed the d7 (early EC) marker panel but was predicted to most closely match d1 (plexus_2), another immature EC cluster (Figure 4C). ECs of several MERFISH clusters mapped to multiple scRNA-seq EC subtypes, suggesting cell heterogeneity. For example, subsets of p2 cells resembled d0 (plexus_1), d1 (plexus_2), d3 (capil-v_brain), and d15 (sinusoid_liver) and subsets of p3 cells resembled d2 (capil-v), d5 (endocardial), d13 (endothelial-to-mesenchymal transition), and d18 (artery_2; Figure 4B). Subclustering on these heterogeneous MERFISH EC clusters revealed cell subsets that scored highest for different scRNA-seq cluster marker panels (Figure 4D through 4J). For example, subclusters p2-2 and p2-5 are mapped to d0 (plexus_1) and p2-3 mapped to d15 (sinusoid_liver); subclusters p3-3 and p3-5 were similar with d18 (artery_2), while p3-2 and p3-4 resembled d5 (endocardial). Collectively, MERFISH clusters showed good correspondence with scRNA-seq clusters (summarized in Figure 4K).

We measured neighborhood enrichment to investigate the spatial correlation of the MERFISH EC clusters. This separated ECs into tissue-specific (≈50% of total ECs analyzed) and widespread EC sets (Figure 5A). Tissue-specific ECs showed the highest enrichment score with themselves and a low score with other clusters (Figure 5A through 5D), while widespread ECs did not show high enrichment scores with themselves and had relatively high scores with several other clusters (Figure 5A, 5E, and 5F). Notably, brain ECs (p4, p6, p9, p12, and p14) were divided into 2 groups: p4, p6, and p12 were widespread within the brain but not at its surface, while p9 and p14 were mostly from the brain surface (Figure 5C). The spatial distributions of the 2 specialized clusters d9 (endothelial-to-immune-like cell transition) and d13 (endothelial-to-mesenchymal transition) were also different: the counterparts of d9 (p0-6 and p18) were widespread without tissue specificity (Figure 5F; Figure S11A), while most d13 (endothelial-to-mesenchymal transition) counterparts showed tissue-specific distributions: p24 (lung and digestive system; Figure 5B), p1-7 and p21 (digestive system; Figure 5D; Figure S11B), and part of p7-3 (lung, digestive system, and kidney; Figure S11F). Subclusters of lung and kidney ECs in p1 had tissue-specific distributions: p1-1/3/4, which mapped to d8:capil_lung, was

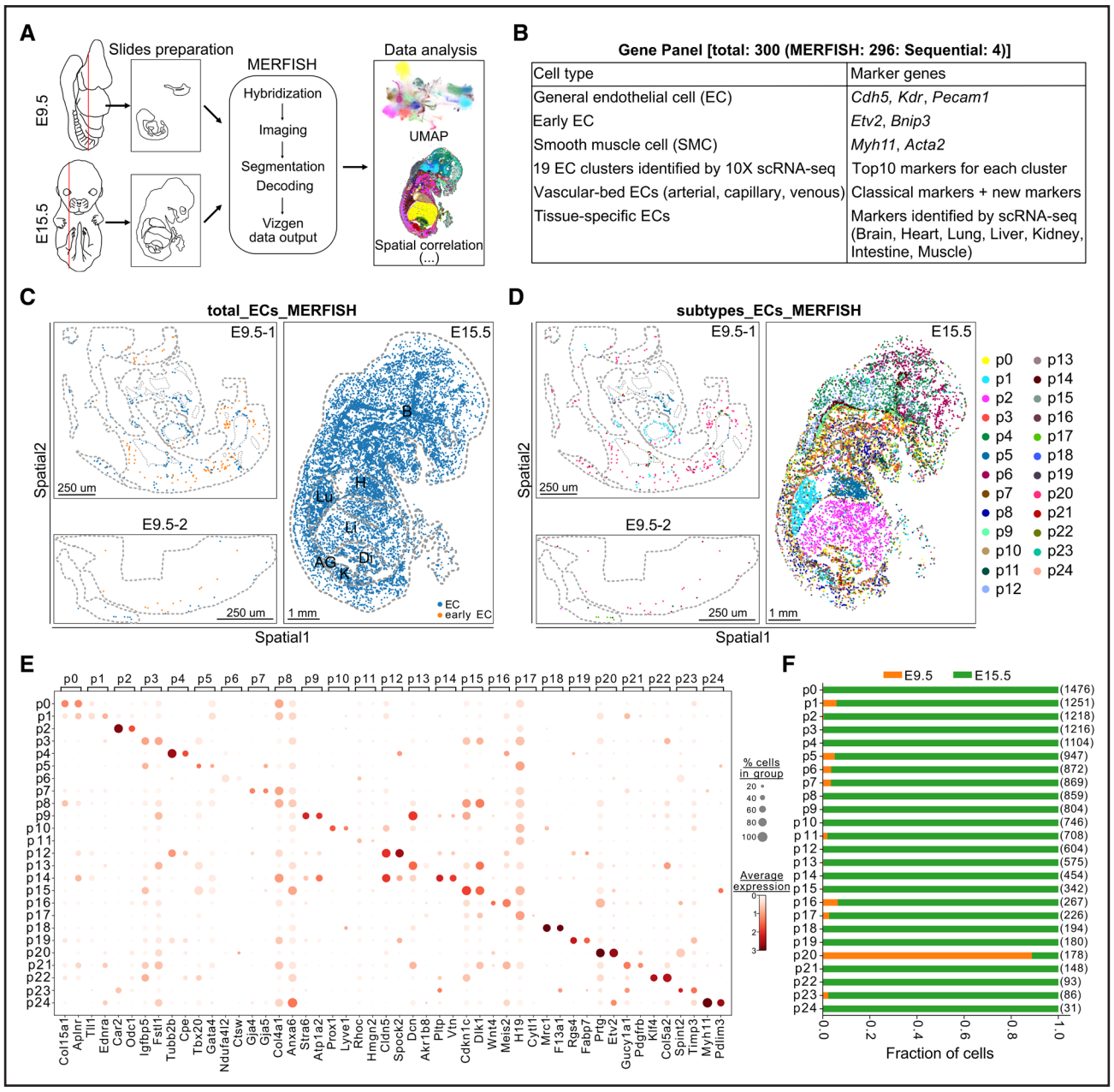

Figure 3. Single-cell spatial transcriptomics map of mouse embryonic endothelial cells (ECs) using multiplexed error-robust fluorescence in situ hybridization (MERFISH).

A, Experimental overview of spatial transcriptomics using the MERFISH platform. Red lines indicate the approximate positions of sample slices. **B**, Composition of the MERFISH panel. **C**, Spatial distribution of ECs and EC progenitors identified from MERFISH data. **D**, Spatial distribution of ECs and EC progenitors annotated by gene expression cluster (designated p for probe-based). **E**, MERFISH clusters can be distinguished from one another by pairs of marker genes. **F**, Distribution of the developmental stage for ECs in each MERFISH cluster. The cell number of each cluster is shown in brackets. AG indicates adrenal gland; B, brain; Di, digestive system; H, heart; K, kidney; Li, liver; and Lu, lung.

located in the lung, and p1-2, corresponding to d2:capil-v, was mostly from the kidney (Figure S11B). Subcluster p2-3, the counterpart of d15 (sinusoid_liver), was specifically distributed in the liver (Figure S11C). Overall p5 was similar to d5 (endocardial; Figure 4), but subclustering revealed that only a subset, p5-1, distributed in the inner part of the heart and closely resembled d5 (endocardial), whereas p5-2 resided in both outer and inner parts of the heart and was more similar to heart vascular ECs (Figure S11E). These results further demonstrate that ECs may become specialized early in embryonic development along with the specialization of organs.

Collectively, we applied orthogonal methods, MERFISH and scRNA-seq, and identified subtypes of embryonic ECs with distinct transcriptome signatures and spatial distributions. The excellent agreement between these approaches demonstrates the reproducibility of our data and analyses and spatially mapped embryonic EC subtypes.

ORIGINAL RESEARCH

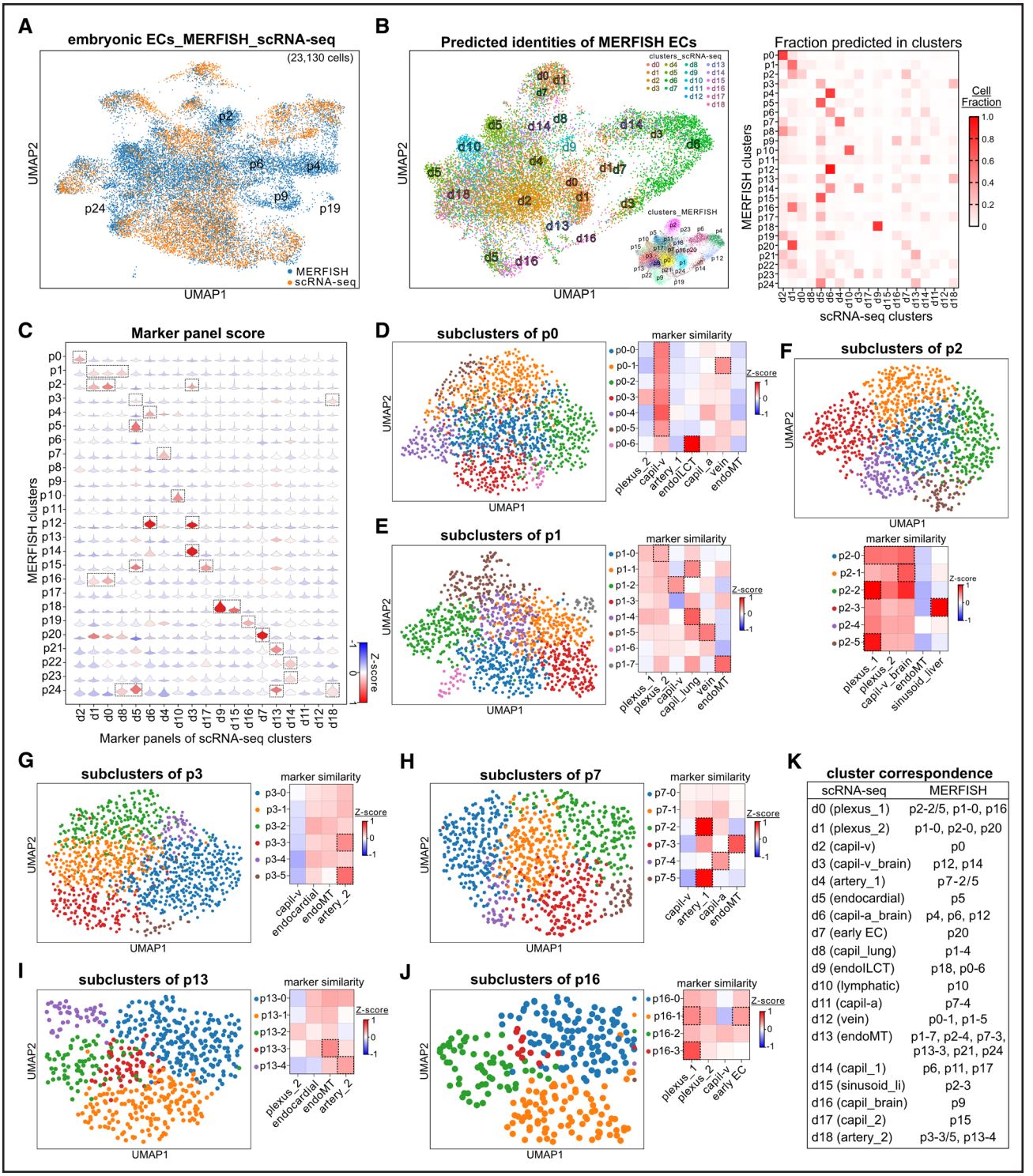

scRNA-seq	MERFISH
d0 (plexus_1)	p2-2/5, p1-0, p16
d1 (plexus_2)	p1-0, p2-0, p20
d2 (capil-v)	p0
d3 (capil-v_brain)	p12, p14
d4 (artery_1)	p7-2/5
d5 (endocardial)	p5
d6 (capil-a_brain)	p4, p6, p12
d7 (early EC)	p20
d8 (capil_lung)	p1-4
d9 (endolLCT)	p18, p0-6
d10 (lymphatic)	p10
d11 (capil-a)	p7-4
d12 (vein)	p0-1, p1-5
d13 (endoMT)	p1-7, p2-4, p7-3, p13-3, p21, p24
d14 (capil_1)	p6, p11, p17
d15 (sinusoid_li)	p2-3
d16 (capil_brain)	p9
d17 (capil_2)	p15
d18 (artery_2)	p3-3/5, p13-4

Figure 4. Correspondence between multiplexed error-robust fluorescence in situ hybridization (MERFISH) and single-cell RNA sequencing (scRNA-seq) clusters.

A, Integrative uniform manifold approximation and projection (UMAP) plot of all endothelial cells (ECs) characterized in scRNA-seq and MERFISH experiments. Unique MERFISH clusters are labeled. **B**, Prediction of MERFISH cell identity from scRNA-seq data (main UMAP) compared with MERFISH cell identities from MERFISH data (inset). Heatmap shows the fraction of cells from MERFISH clusters (rows) predicted to have each scRNA-seq cluster label (columns; **right**). **C**, Enrichment scores of scRNA-seq marker gene panels measured in the MERFISH data set. **D** through **J**, Subclustering of MERFISH EC clusters with high complexity. Adjacent heatmaps show the similarity between MERFISH clusters and scRNA-seq clusters. **K**, Summary of corresponding MERFISH and scRNA-seq clusters.

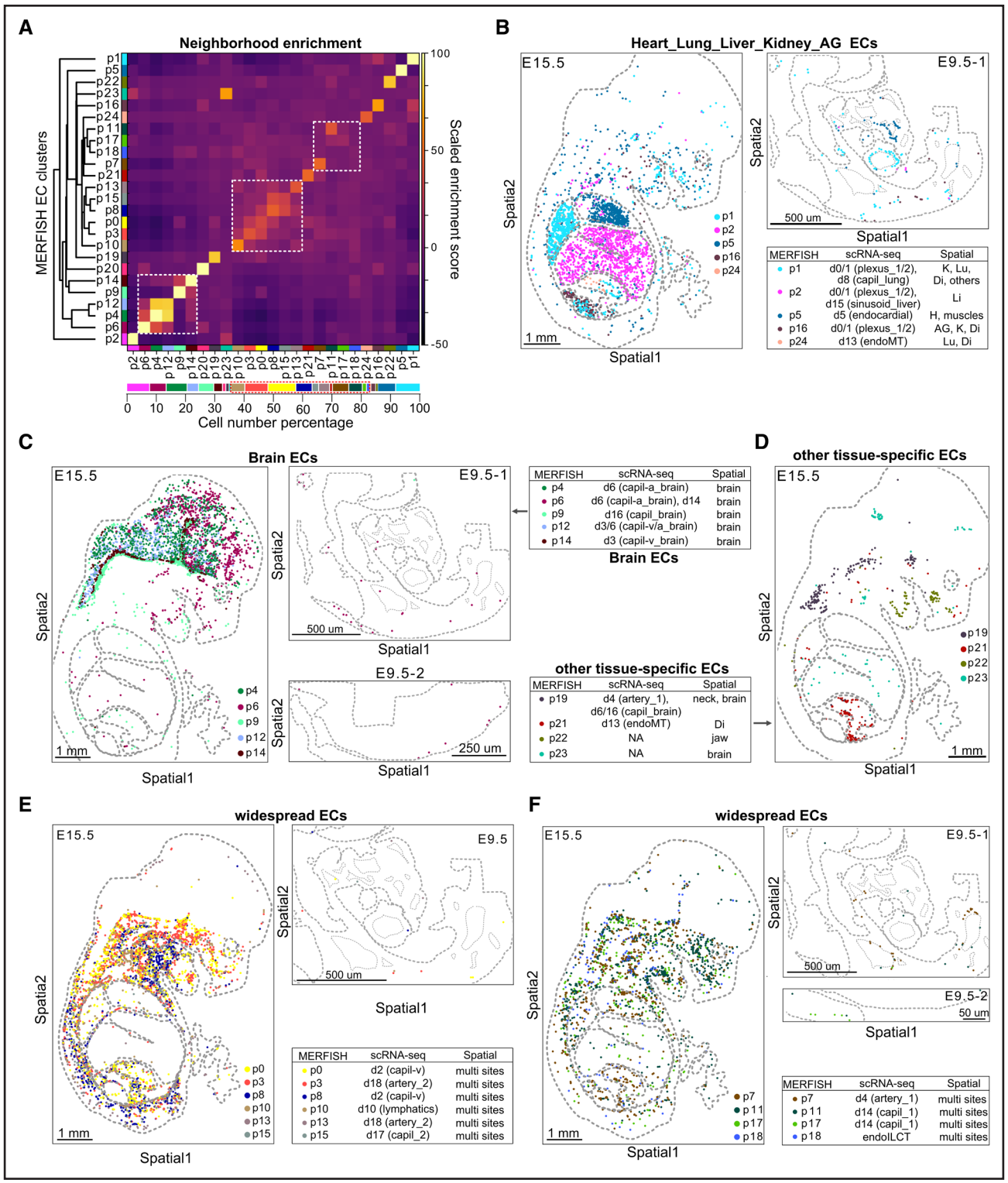

Figure 5. Spatial heterogeneity of mouse embryonic endothelial cells (ECs).
A, Neighborhood enrichment of multiplexed error-robust fluorescence in situ hybridization (MERFISH) EC clusters. The bottom bar plot shows the cell number percentage of each cluster, and the color denotes the cluster identity. **B** through **F**, Spatial distribution of tissue-specific (**B**–**D**) and widespread (**E** and **F**) ECs identified by MERFISH. Tables show the corresponding single-cell RNA sequencing (scRNA-seq) and MERFISH clusters. AG indicates adrenal gland; Di, digestive system; H, heart; K, kidney; Li, liver; Lu, lung; and NA, not applicable.

Next, we used MERFISH data to further characterize the expression of adult tissue-specific EC markers. Markers that we found to be conserved across developmental stages (Figure S6D)—*Slco1c1* and *Spock2* (brain), *Cpe* (heart), *Foxf1* (lung), *Pbx1* (kidney), and *Nkx2*-3 (intestines)—were validated using

the MERFISH data (Figure S12A). We also verified embryonic tissue-specific markers identified in our scRNA-seq data (Figure S12B) and noted that some additional markers of tissue-selective ECs—*Odc1* and *Car2*—were highly enriched in the liver, *Stra6* was most highly expressed in the kidney, and *Casz1* was relatively enriched in muscle tissues (Figure S12C). These results reinforce the establishment of tissue-specific EC subtypes during embryonic development and the dynamic changes of many but not all tissue-specific EC markers between embryonic and adult stages.

Molecular Signatures of Vascular-Bed–Specific ECs

To further understand the differences between ECs from different vascular beds, we focused on clusters that were grouped by vessel type. We aggregated the capillary subtypes (d0, d1, d8, d14, and d17) into a single capillary cluster (capil; Figure 6A). We then analyzed the expression of established arterial-capillary-venous markers across EC subtypes and observed clear patterns (Figure 6B). The capillary cluster showed lower levels of known capillary markers, possibly because this cluster predominantly comprised less mature ECs from plexus_1 (d0) and plexus_2 (d1), which share similar features with EC progenitors (d7; Figures 1G and 2F). *Cxcr4*, *Dll4*, and *Notch1* were highly expressed in artery_1 (d4) and capil-a (d11), while *Jag1* and *Fbln2* were exclusively expressed in artery_2 (d18; Figure 6B). The distinct signatures of these vascular-bed EC types were further highlighted by an analysis of their top 10 marker genes (Figure 6C; Tables S3iii and 4ii). Most of these top markers were specifically expressed in individual types of vessel bed ECs, suggesting their value as vessel bed type markers (Figure 6C and 6D). For example, *Lbp* and *Fam174b* were specifically expressed in vECs (d12), *Dkk2* and *Eln* in artery_2 ECs (d18), *Vegfc* and *Egfl8* in artery_1 (d4; Figure 6D), and *Kcne3* in capil-a (d11), capil, and capil-v (d2; Figure 6D).

EC proliferation and angiogenesis are intrinsic to the rapid growth of the embryonic vasculature. By transcriptome analysis, we assessed the cell-cycle phase of each EC. Most aECs and vECs were in G1 (Figure 6E). A small fraction of cECs were also in G1 (capil_2), but most were in S (plexus_1 and capil-lung) or G2M (plexus_2). Plexus_2 was enriched for cell-cycle–related Gene Ontology (GO) terms, further confirming its proliferative activity (Figure 6F; Table S5ii). Capil_2 was enriched for angiogenic signature genes, indicating that it contained angiogenic ECs (Figure S7F and S7G; Table S5i). Taken together, these results further illustrate the plasticity and heterogeneity of cECs.

To verify these identified markers for aEC-vEC, we explored their expression in our MERFISH data and by targeted RNA in situ hybridization. Arteries and veins, identified by their anatomic positions, were probed for expression of canonical aEC and vEC markers *Gja4* and *Nr2f2*, respectively (Figure 6G; Figure S13A through S13D). *Gja4* was specifically expressed in aECs. *Nr2f2* was highly expressed in vECs, but low levels could also be detected in aECs. In addition, *Nr2f2* was expressed strongly in non-ECs adjacent to vessels (white arrowheads, Figure S13C). Consistent with bioinformatic prediction, *Eln* was specifically and highly expressed in aECs (Figure 6G; Figure S13E). Other predicted aEC genes, *Dkk2*, *Egfl8*, and *Vegfc*, were highly expressed in aECs and lowly expressed in vECs (Figure 6G; Figure S13D and S13F). *Kcne3* was highly expressed in cECs (Figure S13G and S13H). aEC expression of *Vegfc* may provide guidance cues for lymphatics to migrate alongside arteries.[32,33] Unlike arterial markers, most predicted venous markers were not specific. Among the more highly specific vEC markers was *Clec14a* (Figure 6G).

In addition to transcriptional differences, aECs and vECs are also distinguished by their different spatial relationship with vascular SMCs (vSMCs)—arteries have significantly more vSMCs. Therefore, we explored the spatial correlation of ECs and vSMCs with our MERFISH data (Figure S14). Computationally selected SMCs (Figure S8) are grouped into 8 subtypes by their molecular signatures (Figure S14A and S14B). Most SMC subtypes localized to specific organs, whereas a less localized SMC subset was identified as vSMCs (Figure S14C). We then examined the spatial distribution of vascular-bed ECs and SMCs (Figure S14D and S14E). Neighborhood enrichment analysis showed that artery_1 neighbored vSMCs, artery_2, was close to capil-v, capil_2 was close to muscle, capil-a was close to heart SMCs, and plexus_1 was close to liver SMCs (Figure S14F). Spatial plots further verified the spatial correlation and confirmed that artery_1 was mostly derived from big arteries (eg, carotid artery and dorsal aorta), while artery_2 and vein clusters included ECs from both big and small vessels (Figure S14G).

Together, our data show that ECs in different vascular beds can be distinguished with molecular signatures, markers, and spatial distributions identified by our analyses.

Arterialization of Venous-Featured Plexus During Embryonic Arterial Specification

The establishment of aEC and vECs is critical for embryonic vascular development. To identify the steps by which aECs and vECs are specified, we performed developmental lineage trajectory analysis with Slingshot.[34] We excluded capil_1 from this analysis of arteriovenous differentiation because it had transcriptomic features of more mature capillaries rather than of angiogenic ECs and predominantly originated from

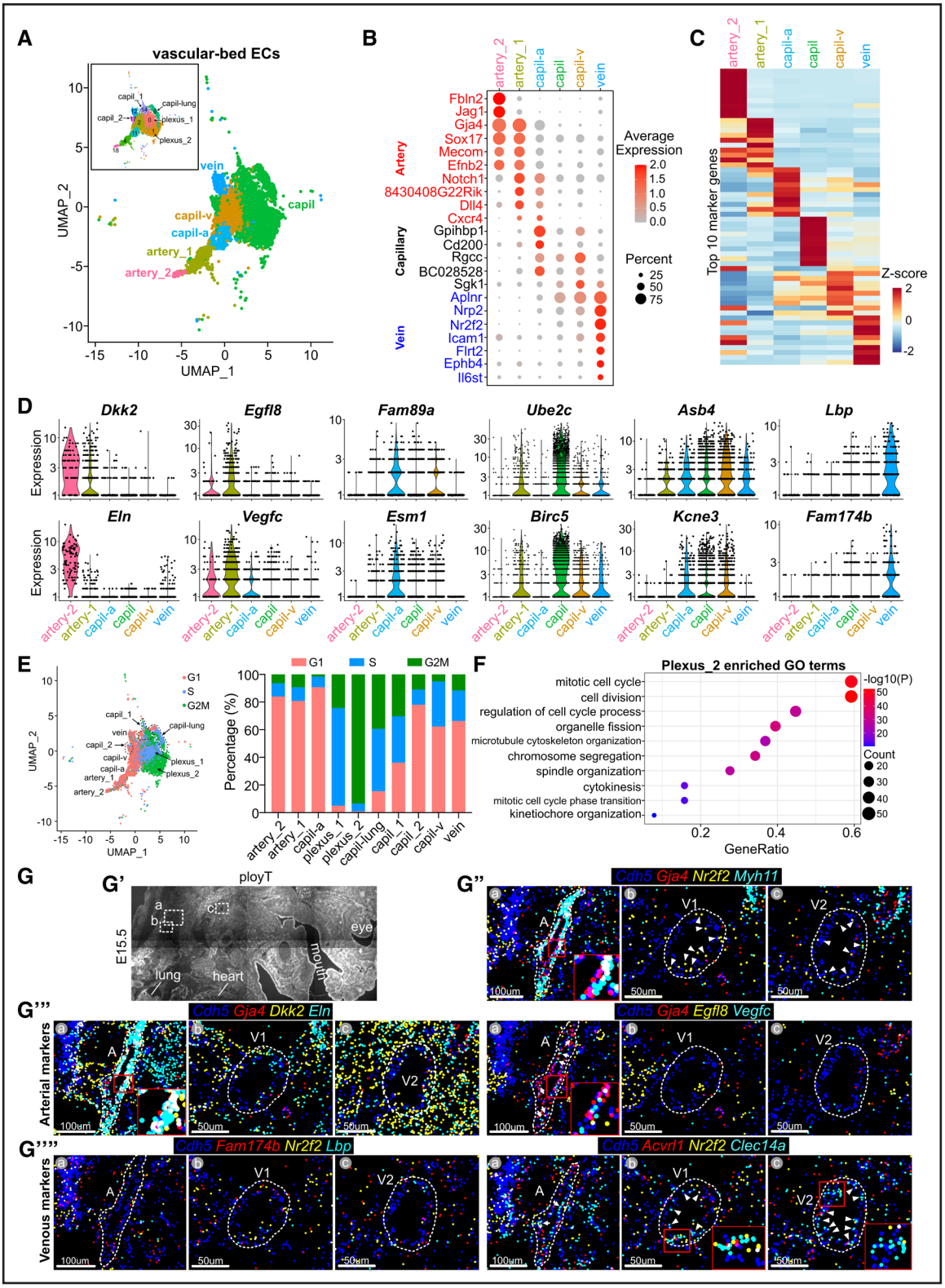

Figure 6. Molecular signatures of vascular-bed–specific endothelial cells (ECs).
A, Uniform manifold approximation and projection (UMAP) plot showing vascular-bed types of embryonic ECs. **B**, Expression of known arterial EC (aEC, red), venous EC (vEC; blue), and capillary (black) marker genes. **C**, Expression of the top 10 marker genes within each EC subtype shown in **A**. **D**, Expression of selected genes that were highly enriched in specific EC subtypes. **E**, Cell-cycle phases in arterial, venous, and capillary ECs (cECs) inferred by transcriptomic analysis. **F**, Top 10 enriched Gene Ontology (GO) terms of cECs in plexus_2. **G**, Sagittal section of E15.5 embryo stained with multiplexed error-robust fluorescence in situ hybridization (MERFISH) probes. Images were captured by the MERFISH imaging platform. G′: polyT staining. G″ to G⁗: MERFISH fluorescent signals, amplified and merged by ImageJ. Arrows and arrowheads highlight higher expression in aECs and vECs, respectively. The anatomic positions of selected artery (A), vein-1 (V1), and vein-2 (V2) (*Continued*)

later-stage embryos (Figures 1E and 2D; Figure S7F). Starting from EC progenitors (d7), the EC developmental tree inferred by Slingshot contained 4 branches: an arterial branch, a venous branch, and branches related to proliferating or specialized cEC subsets (Figure 7A). In the venous trajectory, EC progenitors pass through an immature capillary intermediate state (d0, plexus_1) to form cECs with venous features (d2, capil-v), which then differentiate into vECs (d12) through an angiogenic intermediate state (d17). In the arterial trajectory, EC progenitors follow the same path to form venous-featured cECs (d2, capil-v) and then diverge to differentiate into cECs with arterial features (d11, capil-a) and subsequently into aECs (d4 and d18, artery_1 and artery_2).

This analysis identifies the venous-featured plexus (d2, capil-v) as a lineage decision point, with aEC differentiation occurring through arterialization of venous-featured cECs. Trajectory analysis by another tool, URD,[35] identified similar trajectories between EC progenitors and aECs and vECs, again with d2 (capil-v) as the predominant branch point (Figure S15A and S15B). Independent validation of this trajectory inference came from RNA velocity analysis, which infers cell relationships based on the kinetics of mRNA splicing.[36] RNA velocity results were largely consistent with Slingshot and URD: it identified aEC and vEC trajectories originating from EC progenitors and diverging at venous-featured capillaries (d2, capil-v) to yield aECs and vECs (Figure 7B). Close inspection showed diverging RNA velocity streams within plexus_1 (d0), with some streams crossing a narrow isthmus of venous-featured capillaries (d2, capil-v) to terminate on vECs (d12) and other streams crossing the main body of venous-featured capillaries toward aECs (d11, d4, and d18). Together, the different computational methods define similar arteriovenous differentiation trajectories that proceed from EC progenitors to venous-featured cECs, which further differentiate toward vECs or undergo arterialization to yield aECs.

To validate these trajectories, we analyzed the expression of representative aEC and vEC marker genes along the arterial and venous differentiation pseudotime. Over the aEC trajectory, we observed upregulation of established aEC marker genes, *Efnb2*, *Sox17*, *Gja4*, *Dll4*, and *Mecom*, and downregulation of vEC marker genes, *Ephb4*, *Nr2f2*, *Nrp2*, and *Flrt2* (Figure 7C). In contrast, we observed the opposite pattern during vEC development pseudotime. Notch pathway activation, which promotes arterial differentiation, was observed in aEC but not vEC differentiation (Figure S15C). Consistent with our earlier cell-cycle activity analysis, cell-cycle marker expression declined during both arterial and venous trajectories (Figure S15D). These analyses further validated the inferred aEC and vEC differentiation trajectories.

Next, we scored each cell for arterial or venous character based on their expression of known marker genes. EC progenitors and cECs exhibited venous character, which increased during venous differentiation pseudotime (Figure 7C; Figure S15E). In contrast, arterial character increased following bifurcation of the arterial trajectory at d2 (capil-v). This analysis further highlights the arterialization of venous-featured ECs during arterial differentiation.

We then investigated the dynamic transcriptional features of embryonic arteriovenous differentiation. Eight major gene modules (M1–M8) along the arterial and venous differentiation paths were identified based on differential gene analyses (Figure 7D). Module 6 genes were most highly expressed in the capil-v state and showed enrichment of signaling pathways involved in cell death, herpesvirus infection, and protein phosphorylation (Figure 7D and 7E; Table S5iii), suggesting that these genes regulate this special intermediate state of arteriovenous differentiation.

To further verify the arteriovenous trajectories, we integrated our data set (E9.5, E12.5, and E15.5) with a data set by Hou et al[7] (E9.0 and E10.0) from the same microdroplet platform to expand the cell number and the coverage of the developmental stages and the number of cells (Figure 7F). cECs (plexus_1, plexus_2, and capil_lung) from the current data set intermingled well with the cells annotated by Hou et al as venous VEC (Figure 7F, left) and also functioned as an intermediate following progenitor ECs for arteriovenous specification (Figure 7F, right). Moreover, trajectory analysis showed that both large artery ECs (artery_1 and artery_2) and ECs annotated as arterial plexus ECs (Vwa1+VEC) by Hou et al. differentiated from venous cECs (capil-v; Figure 7F, right). These analyses further validated the arterialization of venous-featured cEC during embryonic arterial development.

Transcriptional Regulation of Arteriovenous Differentiation

To study the underlying molecular mechanisms driving arteriovenous differentiation, we used single-cell regulatory network inference and clustering, which identifies regulons (groups of genes coregulated by the same TF) based on gene coexpression network analysis, TF motif enrichment, and TF expression.[37] Single-cell regulatory network inference and clustering analysis predicted that different regulons predominate in different EC subtypes (Figure 8A). For instance, ETV2 and ETS1 regulon

Figure 6 Continued. are marked by dotted lines. G′: classical arterial and venous markers confirmed the arteriovenous identities of selected vessels. G″ and G‴: newly identified arterial and venous marker genes, respectively. Capil indicates capillary EC (cEC; union of capil-lung, capil_1, capil_2, plexus_1, and plexus_2); capil-a, capillary arterial EC; and capil-v, capillary venous EC.

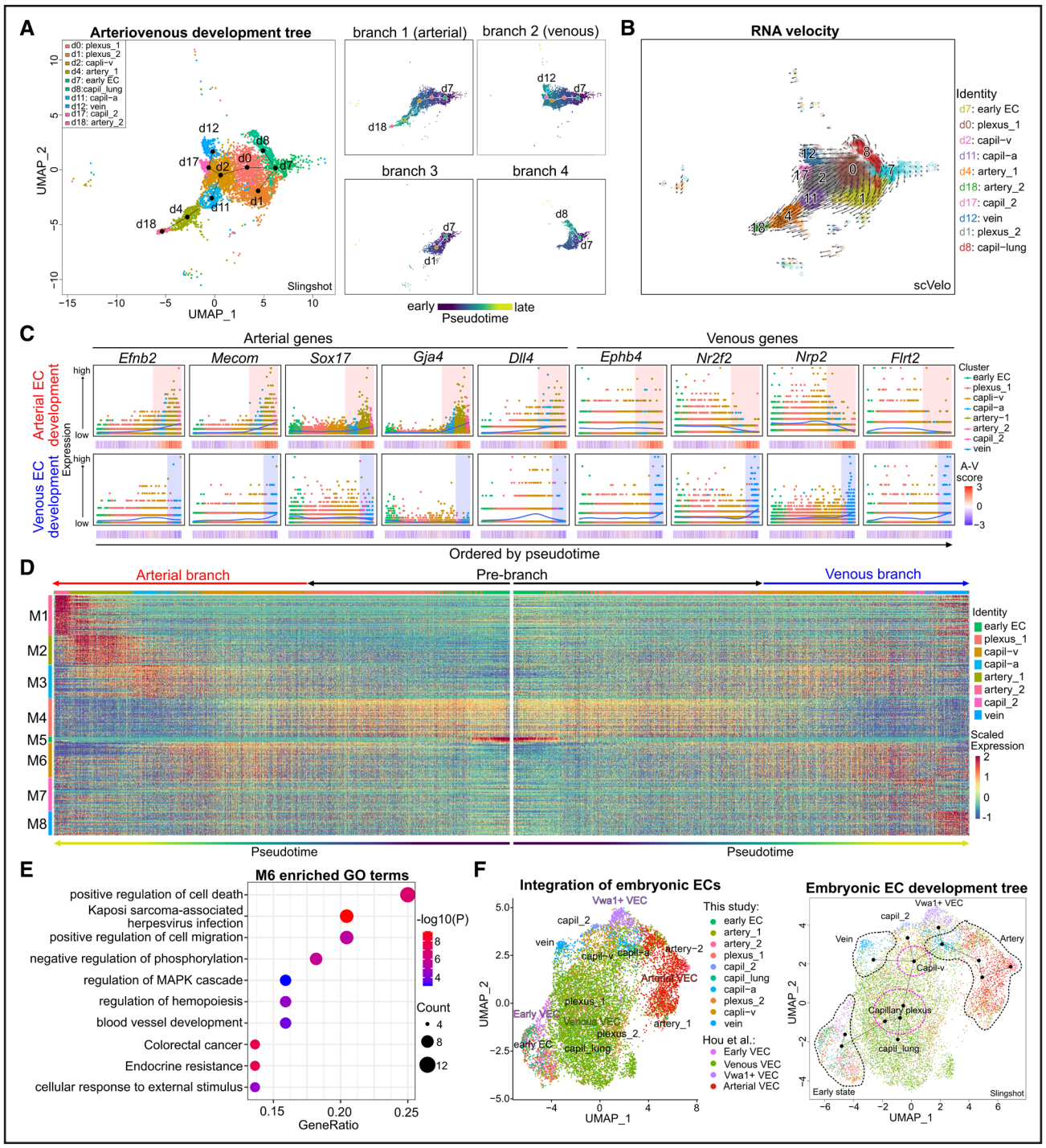

Figure 7. Developmental cell lineage tree of embryonic arteriovenous differentiation.

A, Trajectory of arteriovenous differentiation inferred by Slingshot. **B**, RNA velocity vector field displayed on the uniform manifold approximation and projection (UMAP) plot. A randomly selected early endothelial cell (EC) was specified as the starting point. **C**, Expression of the indicated venous and arterial marker genes along the arterial and venous differentiation paths inferred by Slingshot. Cells are ordered on the *x* axis by differentiation pseudotime. Arteriovenous scores are shown at the bottom of each plot. Red and blue shading toward the right-hand side of each plot indicates arterial ECs (aECs) and venous ECs (vECs), respectively. **D**, Gene expression during the Slingshot arteriovenous differentiation trajectory. Eight major gene modules (M) were identified, with peak expression in arteries (M1 and M2), capil-a (M3), early EC and capillary plexus (M4), early EC (M5), capil-v (M6), capil_2 (M7), and vein (M8). **E**, The top 10 enriched Gene Ontology (GO) terms for M6, in which gene expression peaks in capil-v, the cluster at the bifurcation of aEC and vEC trajectories. **F**, Cell trajectory of embryonic EC development built by integrating data from this study and the single-cell RNA sequencing (scRNA-seq) data from reference [7] (**left**) Cells colored by their clustering in this study or reference [7]. (**right**) Slingshot trajectory based on the integrated data set.

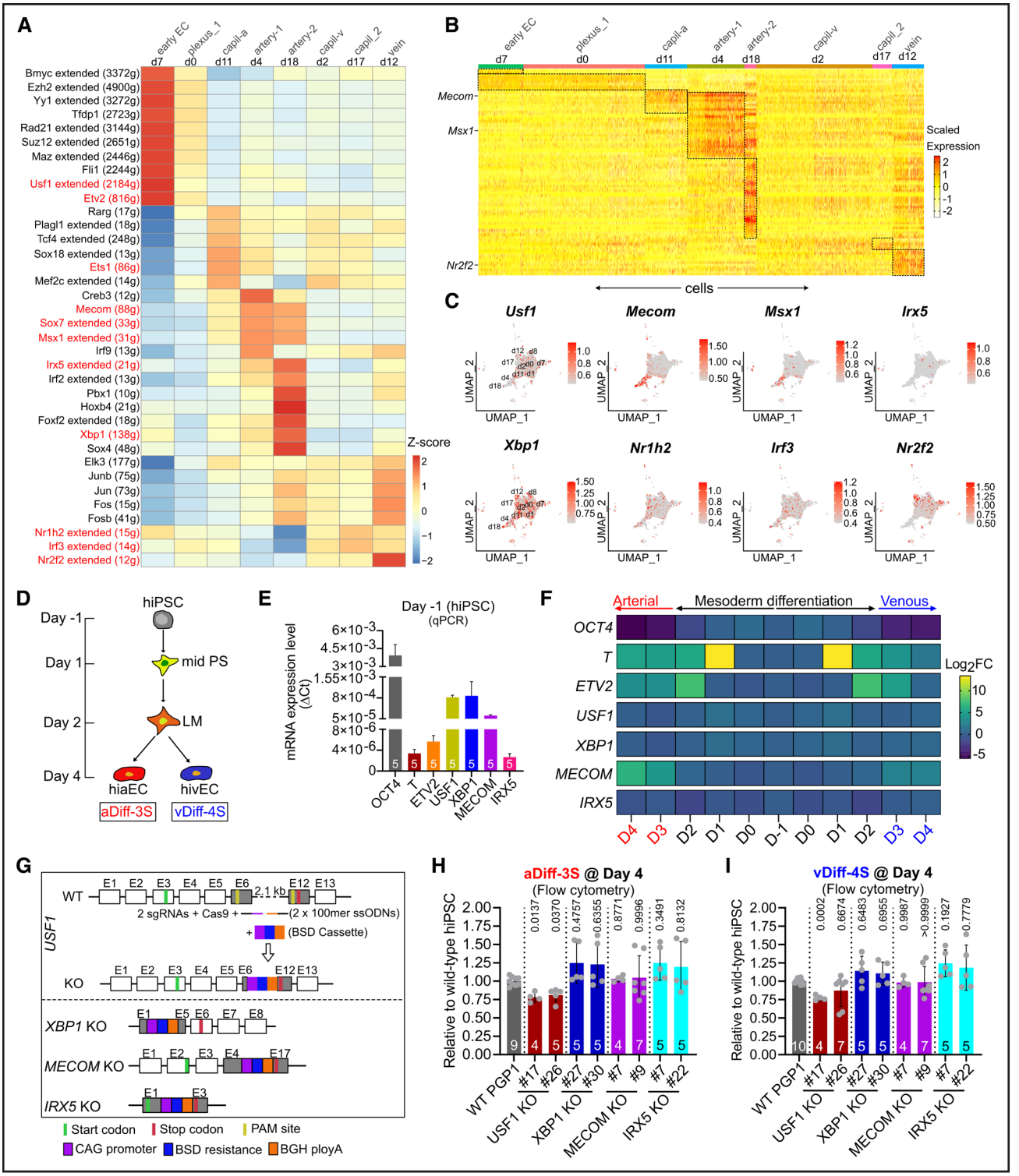

Figure 8. Transcriptional regulation of arteriovenous differentiation.

A, Transcription factor (TF) gene-regulatory networks inferred by single-cell regulatory network inference and clustering. Columns: individual endothelial cell (EC) clusters. Rows: extended TF regulons. Selected regulons mentioned in the text are highlighted. **B**, TF expression in each cluster. Each row represents 1 TF and each column represents 1 cell, grouped by EC cluster. Representative TFs are highlighted. **C**, Expression of selected TFs in arteriovenous clusters. **D**, Schematic of iPSC platform for differentiation into human-induced pluripotent stem cell (hiPSC)-arterial EC (aECs; aDiff-3S) or hiPSC-venous ECs (vECs; vDiff-4S). Modified from Ang et al[38] with permission. **E**, Quantitative reverse transcription PCR (RT-qPCR) showing expression of selected TFs at day 1 (hiPSC), the start point of differentiation. **F**, Expression of selected TFs during hiPSC-aEC and hiPSC-vEC differentiation. D-1 serves as the starting point. **G**, Gene targeting strategies to knockout (KO) *USF1*, *XBP1*, *MECOM*, and *IRX5* in iPSCs. **H** and **I**, Quantification of hiPSC-aEC and hiPSC-vEC differentiation efficiencies of wild-type (WT) and KO hiPSCs as quantified by flow cytometry at day 4. Numbers indicate *P* values (ANOVA with the Dunnett multiple comparison test compared with wild type). (*Continued*)

activities were upregulated in early ECs (d7) and capilla (d11), respectively, whereas an SOX7 network was enriched in artery_1 and artery_2 (d4 and d18), and vECs (d12) showed increased activity of an NR2F2 network. These predictions are consistent with known functions of these TFs in EC and arteriovenous specification.[20,23,24,39] *Mecom*, recently reported to regulate arteriovenous differentiation, was predicted to regulate arterial clusters.[40] Unexpected TF regulons identified included USF1 in early ECs; MSX1, IRX5, and XBP1 in arterial clusters; and IRF3 and NR1H2 in venous clusters (Figure 8A).

To further investigate TFs that govern arteriovenous differentiation, we analyzed the TF markers of embryonic EC subtypes. Each embryonic EC class expressed a distinct TF set (Figure 8B; Table S6). For example, aECs more highly expressed *Mecom* and *Msx1* and vECs *Nr2f2* (Figure 8B and 8C). The expression patterns of several of the TFs implicated by single-cell regulatory network inference and clustering to regulate arteriovenous differentiation did not show selective expression in expected EC subtypes: *Usf1*, *Xbp1*, *Nr1h2*, and *Irf3* were widely expressed, and *Irx5* was not detected (Figure 8C).

To mechanistically study arteriovenous differentiation, we differentiated human-induced pluripotent stem cells (hiPSCs) into aECs or vECs[38] (hiPSC-aECs and hiPSC-vECs; Figure 8D). In this system, we profiled single-cell regulatory network inference and clustering candidate genes *MECOM*, *IRX5*, *USF1*, and *XBP1* and control genes *OCT4*, *T* (Brachyury), and *ETV2* by RT-qPCR (Figure 8E and 8F). As expected, stem cell marker *OCT4* was highly expressed in iPSCs and subsequently downregulated, and expression of EC progenitor marker *ETV2* peaked at day 2, just before arteriovenous differentiation. *USF1* and *XBP1* were robustly expressed at all stages with a peak at day 1. *MECOM* increased in both hiPSC-aECs and hiPSC-vECs but reached higher levels in hiPSC-aECs. *IRX5* was nearly undetectable in EC lineages. These expression patterns suggested that *USF1* and *XBP1* may function in EC differentiation and *Mecom* may participate more in arterial differentiation.

To test the requirement of *USF1*, *XBP1*, *MECOM*, and *IRX5* in EC differentiation, we used CRISPR (clustered regularly interspaced short palindromic repeats) genome editing to create knockout hiPSC lines (Figure 8G). For each gene, we isolated 2 knockout clones (Figure S16). Then, we differentiated the clonal lines and measured hiPSC-aEC and hiPSC-vEC differentiation efficiencies on day 4. *IRX5*, *MECOM*, or *XBP1* knockout did not impair either hiPSC-aEC or hiPSC-vEC differentiation. Ablation of *USF1* consistently reduced hiPSC-aEC differentiation efficiency in 2 different hiPSC clones, but its inhibitory effect on venous differentiation varied between clonal lines (Figure 8H and 8I). Collectively, these data demonstrated *USF1* functions in efficient hiPSC-aEC differentiation. Further work will be needed to test its role in arteriovenous specification in vivo.

DISCUSSION

We established a single-cell transcriptome map of embryonic ECs during key stages of vascular development, identified 19 distinct EC subtypes, and mapped their spatial distribution. Our study provides novel insights into arteriovenous differentiation and the sources of endothelial heterogeneity during embryonic development.

Tissue origin and vessel type are major determinants of EC heterogeneity. Among adult ECs, heterogeneity primarily arises from tissue rather than vessel-type specificity.[3] A prior study of E14.5 embryos also concluded that ECs group by their tissue origins[6] but this study did not verify the embryonic expression patterns of adult tissue-specific markers used to reach this conclusion. Another scRNA-seq study of E8-E11 embryos showed that ECs from different parts of the embryo, except the yolk sac, intermingle with each other and cluster by vessel type.[7] We curated tissue-specific EC markers and then characterized their expression in embryonic and adult ECs from individual tissues. Only a subset of adult tissue-specific EC markers had similar specificity in embryonic ECs. Moreover, only a small subset of embryonic ECs were grouped by their tissue origin, while most were grouped by vessel type. Spatial transcriptomics validated these analyses and demonstrated that most embryonic ECs fall into a widespread category that is not defined by tissue-specific markers. Together, these data demonstrate that vascular-bed heterogeneity predominantly contributes to embryonic EC heterogeneity. This suggests that murine tissue-specific EC differentiation mostly occurs after E15.5, during late organ development.

Marker genes are vital for biologists to study different cell types. Several markers of aECs and vECs have been described.[41] Arterial markers such as *Dll4* and *Gja4* are generally robust and were validated in embryonic ECs by this study. However, classical venous markers are often less specific. For example, *Ephb4*, *Nrp2*, and *Nr2f2* are also highly expressed in lymphatic ECs and can be detected in some early ECs, cECs, and aECs. Here, we identified and validated new embryonic vEC markers *Lbp*, *Fam174b*, and *Clec14a* and cEC marker *Kcne3*. In addition, we identified tissue-specific EC markers that are conserved between embryonic and adult stages (eg, *Slc2a1* [brain], *Foxf1* [lung], *Pbx1* [kidney], and *Nkx2-3* [small intestine], respectively) or are specific for embryonic stages (eg, *Slc38a5* [brain], *Hand2* [heart],

Figure 8 Continued. Each point represents an independent differentiation sample. BSD indicates blasticidin; BGH polyA, the bovine growth hormone polyadenylation; CAG promoter, the cytomegalovirus (CMV) enhancer fused to the chicken beta-actin promoter; LM, lateral mesoderm; PAM, protospacer adjacent motif; and mid PS, mid primitive streak.

and *Stab2* [liver]). These markers will facilitate the further study of ECs.

The cellular origins of aECs and vECs remain controversial. Lineage tracing studies at early embryonic stages demonstrated that aECs and vECs develop from different progenitors with different embryonic positions and stages.[8,9] Developing zebrafish cardinal veins arise from the dorsal aorta,[42] whereas a subset of aECs in developing heart, brain, and retina develops from vECs through a fate conversion.[10–13] Here, by single-cell sequencing of E9.5 to E15.5 embryos, we captured ECs at different states of arteriovenous differentiation, including precursors, intermediate plexus, and immature and mature capillary, artery, and vein ECs. We integrated these data with previously published data from earlier embryos to construct complete differentiation trajectories from early EC progenitors to mature aECs and vECs. Both aEC and vEC developmental paths proceed through a special capillary plexus state with venous characteristics and high proliferative potential. This venous capillary plexus state is a branch point. One branch leads to mature vECs. A second branch leads to mature aECs, suggesting that arterialization of a venous-featured capillary plexus is the predominant pathway for arterial specification in the mouse embryo, consistent with a study of E8 to E11 embryos[7] that identified venous arterialization as a source for a subset of aECs. Together, this study reveals a more complete and detailed model for embryonic arteriovenous differentiation.

Prior studies of signaling pathways and transcriptional mechanisms that govern arterial and venous specification identified Notch and high VEGFA (vascular endothelial growth factor A) as critical for arterial specification, while BMP signaling and NR2F2 are vital for venous specification.[15,17,20,43,44] This study revealed the transcriptional dynamics of arterial and venous specification and the expression pattern and regulons of TF enriched along aEC and vEC differentiation trajectories. These analyses predicted novel transcriptional regulators of arteriovenous specification. We tested these predictions in a hIPSC to aEC or vEC differentiation system. These experiments showed that USF1, a widely expressed TF, promotes effective aEC specification. However, USF1 knockout mice do not have overt vascular development defects,[45] possibly due to genetic compensation by other factors such as USF2. Further studies to interrogate USF1 function in vivo are warranted.

Some limitations of this study are that we dissociated whole embryos for scRNA-seq rather than individual tissues. Our approach minimized the batch effect between tissues but may have limited our sensitivity to tissue-specific differences. Our analyses focused on integrative analyses across developmental stages. This strategy allowed us to analyze cells from multiple developmental time points at once and use them to build a cohesive arteriovenous differentiation trajectory but may have reduced sensitivity for stage-specific changes in gene expression or cell states.

CONCLUSIONS

Our results provide a spatiotemporal map of embryonic EC heterogeneity at single-cell resolution and demonstrate that the diversity of ECs in the embryo arises from both tissue origin and vascular-bed position. Developing aECs and vECs share common venous-featured capillary precursors and are regulated by distinct transcriptional regulatory networks.

ARTICLE INFORMATION

Received November 6, 2023; revision received January 28, 2024; accepted January 30, 2024.

Affiliations

Department of Cardiology, Boston Children's Hospital, Boston, MA (Jian Chen, X.Z., M.A.T., S.S., F.X., Jiehui Chen, P.Z., W.T.P.). Department of Genetics, Harvard Medical School, Boston, MA (D.M.D., C.E.S., J.G.S.). Division of Cardiovascular Medicine, Brigham and Women's Hospital, Boston, MA (C.E.S.). Howard Hughes Medical Institute, Chevy Chase, MD (C.E.S.). Harvard Stem Cell Institute, Cambridge, MA (W.T.P.).

Acknowledgments

The authors are grateful to members of the Pu Laboratory for their expertise and critical discussion.

Author Contributions

F. Xiao constructed a *Mecom* knockout human-induced pluripotent stem cell line. P. Zhou provided reagents and discussion. Jian Chen and X. Zhang wrote the article, and it was edited by C.E. Seidman, J.G. Seidman, and W.T. Pu. W.T. Pu supervised the study. Jian Chen and W.T. Pu designed the study. Jian Chen performed the experiments and analyzed the data. X. Zhang and Jiehui Chen performed computational analysis. D. Morris DeLaughter prepared 10× genomics single-cell libraries and performed sequencing. Jian Chen and M.A. Trembley prepared the sample for a multiplexed error-robust fluorescence in situ hybridization study (MERFISH). M.A. Trembley and S. Saifee performed MERFISH experiments.

Sources of Funding

This study was supported by National Institutes of Health (R01 HL138571 and R01 HL151450).

Disclosures

None.

Supplemental Material

Expanded Materials and Methods
Figures S1–S16
Tables S1–S8
References 46–56

REFERENCES

1. Marziano C, Genet G, Hirschi KK. Vascular endothelial cell specification in health and disease. *Angiogenesis*. 2021;24:213–236. doi: 10.1007/s10456-021-09785-7
2. Fish JE, Wythe JD. The molecular regulation of arteriovenous specification and maintenance. *Dev Dyn*. 2015;244:391–409. doi: 10.1002/dvdy.24252
3. Kalucka J, de Rooij LPMH, Goveia J, Rohlenova K, Dumas SJ, Meta E, Conchinha NV, Taverna F, Teuwen LA, Veys K, et al. Single-cell transcriptome atlas of murine endothelial cells. *Cell*. 2020;180:764–779.e20. doi: 10.1016/j.cell.2020.01.015

4. Paik DT, Tian L, Williams IM, Rhee S, Zhang H, Liu C, Mishra R, Wu SM, Red-Horse K, Wu JC. Single-cell RNA sequencing unveils unique transcriptomic signatures of organ-specific endothelial cells. *Circulation*. 2020;142:1848–1862. doi: 10.1161/CIRCULATIONAHA.119.041433
5. Nolan DJ, Ginsberg M, Israely E, Palikuqi B, Poulos MG, James D, Ding BS, Schachterle W, Liu Y, Rosenwaks Z, et al. Molecular signatures of tissue-specific microvascular endothelial cell heterogeneity in organ maintenance and regeneration. *Dev Cell*. 2013;26:204–219. doi: 10.1016/j.devcel.2013.06.017
6. Guo FH, Guan YN, Guo JJ, Zhang LJ, Qiu JJ, Ji Y, Chen AF, Jing Q. Single-cell transcriptome analysis reveals embryonic endothelial heterogeneity at spatiotemporal level and multifunctions of MicroRNA-126 in mice. *Arterioscler Thromb Vasc Biol*. 2022;42:326–342. doi: 10.1161/ATVBAHA.121.317093
7. Hou S, Li Z, Dong J, Gao Y, Chang Z, Ding X, Li S, Li Y, Zeng Y, Xin Q, et al. Heterogeneity in endothelial cells and widespread venous arterialization during early vascular development in mammals. *Cell Res*. 2022;32:333–348. doi: 10.1038/s41422-022-00615-z
8. Chong DC, Koo Y, Xu K, Fu S, Cleaver O. Stepwise arteriovenous fate acquisition during mammalian vasculogenesis. *Dev Dyn*. 2011;240:2153–2165. doi: 10.1002/dvdy.22706
9. Kohli V, Schumacher JA, Desai SP, Rehn K, Sumanas S. Arterial and venous progenitors of the major axial vessels originate at distinct locations. *Dev Cell*. 2013;25:196–206. doi: 10.1016/j.devcel.2013.03.017
10. Red-Horse K, Ueno H, Weissman IL, Krasnow MA. Coronary arteries form by developmental reprogramming of venous cells. *Nature*. 2010;464:549–553. doi: 10.1038/nature08873
11. Xu C, Hasan SS, Schmidt I, Rocha SF, Pitulescu ME, Bussmann J, Meyen D, Raz E, Adams RH, Siekmann AF. Arteries are formed by vein-derived endothelial tip cells. *Nat Commun*. 2014;5:5758. doi: 10.1038/ncomms6758
12. Bussmann J, Wolfe SA, Siekmann AF. Arterial-venous network formation during brain vascularization involves hemodynamic regulation of chemokine signaling. *Development*. 2011;138:1717–1726. doi: 10.1242/dev.059881
13. Fujita M, Cha YR, Pham VN, Sakurai A, Roman BL, Gutkind JS, Weinstein BM. Assembly and patterning of the vascular network of the vertebrate hindbrain. *Development*. 2011;138:1705–1715. doi: 10.1242/dev.058776
14. Su T, Stanley G, Sinha R, D'Amato G, Das S, Rhee S, Chang AH, Poduri A, Raftrey B, Dinh TT, et al. Single-cell analysis of early progenitor cells that build coronary arteries. *Nature*. 2018;559:356–362. doi: 10.1038/s41586-018-0288-7
15. Lawson ND, Vogel AM, Weinstein BM. sonic hedgehog and vascular endothelial growth factor act upstream of the Notch pathway during arterial endothelial differentiation. *Dev Cell*. 2002;3:127–136. doi: 10.1016/s1534-5807(02)00198-3
16. Krebs LT, Xue Y, Norton CR, Shutter JR, Maguire M, Sundberg JP, Gallahan D, Closson V, Kitajewski J, Callahan R, et al. Notch signaling is essential for vascular morphogenesis in mice. *Genes Dev*. 2000;14:1343–1352. doi: 10.1101/gad.14.11.1343
17. Neal A, Nornes S, Payne S, Wallace MD, Fritzsche M, Louphrasitthiphol P, Wilkinson RN, Chouliaras KM, Liu K, Plant K, et al. Venous identity requires BMP signalling through ALK3. *Nat Commun*. 2019;10:453. doi: 10.1038/s41467-019-08315-w
18. Chavkin NW, Genet G, Poulet M, Jeffery ED, Marziano C, Genet N, Vasavada H, Nelson EA, Acharya BR, Kour A, et al. Endothelial cell cycle state determines propensity for arterial-venous fate. *Nat Commun*. 2022;13:5891. doi: 10.1038/s41467-022-33324-7
19. Luo W, Garcia-Gonzalez I, Fernández-Chacón M, Casquero-Garcia V, Sanchez-Muñoz MS, Mühleder S, Garcia-Ortega L, Andrade J, Potente M, Benedito R. Arterialization requires the timely suppression of cell growth. *Nature*. 2021;589:437–441. doi: 10.1038/s41586-020-3018-x
20. You LR, Lin FJ, Lee CT, DeMayo FJ, Tsai MJ, Tsai SY. Suppression of notch signalling by the COUP-TFII transcription factor regulates vein identity. *Nature*. 2005;435:98–104. doi: 10.1038/nature03511
21. Seo S, Fujita H, Nakano A, Kang M, Duarte A, Kume T. The forkhead transcription factors, Foxc1 and Foxc2, are required for arterial specification and lymphatic sprouting during vascular development. *Dev Biol*. 2006;294:458–470. doi: 10.1016/j.ydbio.2006.03.035
22. Corada M, Orsenigo F, Morini MF, Pitulescu ME, Bhat G, Nyqvist D, Breviario F, Conti V, Briot A, Iruela-Arispe ML, et al. Sox17 is indispensable for acquisition and maintenance of arterial identity. *Nat Commun*. 2013;4:2609. doi: 10.1038/ncomms3609
23. Kataoka H, Hayashi M, Nakagawa R, Tanaka Y, Izumi N, Nishikawa S, Jakt ML, Tarui H, Nishikawa SI. Etv2/ER71 induces vascular mesoderm from Flk1+PDGFRα+ primitive mesoderm. *Blood*. 2011;118:6975–6986. doi: 10.1182/blood-2011-05-352658
24. Sumanas S, Lin S. Ets1-related protein is a key regulator of vasculogenesis in zebrafish. *PLoS Biol*. 2006;4:e10. doi: 10.1371/journal.pbio.0040010
25. Gustavsson C, Agardh CD, Zetterqvist AV, Nilsson J, Agardh E, Gomez MF. Vascular cellular adhesion molecule-1 (VCAM-1) expression in mice retinal vessels is affected by both hyperglycemia and hyperlipidemia. *PLoS One*. 2010;5:e12699. doi: 10.1371/journal.pone.0012699
26. Yamamoto K, de Waard V, Fearns C, Loskutoff DJ. Tissue distribution and regulation of murine von Willebrand factor gene expression in vivo. *Blood*. 1998;92:2791–2801. doi: 10.1182/blood.V92.8.2791
27. Andueza A, Kumar S, Kim J, Kang DW, Mumme HL, Perez JI, Villa-Roel N, Jo H. Endothelial reprogramming by disturbed flow revealed by single-cell RNA and chromatin accessibility study. *Cell Rep*. 2020;33:108491. doi: 10.1016/j.celrep.2020.108491
28. Yang Y, Oliver G. Development of the mammalian lymphatic vasculature. *J Clin Invest*. 2014;124:888–897. doi: 10.1172/JCI71609
29. Srinivasan RS, Dillard ME, Lagutin OV, Lin FJ, Tsai S, Tsai MJ, Samokhvalov IM, Oliver G. Lineage tracing demonstrates the venous origin of the mammalian lymphatic vasculature. *Genes Dev*. 2007;21:2422–2432. doi: 10.1101/gad.1588407
30. Chen KH, Boettiger AN, Moffitt JR, Wang S, Zhuang X. Spatially resolved, highly multiplexed RNA profiling in single cells. *Science*. 2015;348:aaa6090. doi: 10.1126/science.aaa6090
31. Hie B, Bryson B, Berger B. Efficient integration of heterogeneous single-cell transcriptomes using Scanorama. *Nat Biotechnol*. 2019;37:685–691. doi: 10.1038/s41587-019-0113-3
32. Bussmann J, Bos FL, Urasaki A, Kawakami K, Duckers HJ, Schulte-Merker S. Arteries provide essential guidance cues for lymphatic endothelial cells in the zebrafish trunk. *Development*. 2010;137:2653–2657. doi: 10.1242/dev.048207
33. Vaahtomeri K, Karaman S, Mäkinen T, Alitalo K. Lymphangiogenesis guidance by paracrine and pericellular factors. *Genes Dev*. 2017;31:1615–1634. doi: 10.1101/gad.303776.117
34. Street K, Risso D, Fletcher RB, Das D, Ngai J, Yosef N, Purdom E, Dudoit SS. Slingshot: cell lineage and pseudotime inference for single-cell transcriptomics. *BMC Genomics*. 2018;19:477. doi: 10.1186/s12864-018-4772-0
35. Farrell JA, Wang Y, Riesenfeld SJ, Shekhar K, Regev A, Schier AF. Single-cell reconstruction of developmental trajectories during zebrafish embryogenesis. *Science*. 2018;360:eaar3131. doi: 10.1126/science.aar3131
36. La Manno G, Soldatov R, Zeisel A, Braun E, Hochgerner H, Petukhov V, Lidschreiber K, Kastriti ME, Lönnerberg P, Furlan A, et al. RNA velocity of single cells. *Nature*. 2018;560:494–498. doi: 10.1038/s41586-018-0414-6
37. Aibar S, González-Blas CB, Moerman T, Huynh-Thu VA, Imrichova H, Hulselmans G, Rambow F, Marine JC, Geurts P, Aerts J, et al. SCENIC: single-cell regulatory network inference and clustering. *Nat Methods*. 2017;14:1083–1086. doi: 10.1038/nmeth.4463
38. Ang LT, Nguyen AT, Liu KJ, Chen A, Xiong X, Curtis M, Martin RM, Raftry BC, Ng CY, Vogel U, et al. Generating human artery and vein cells from pluripotent stem cells highlights the arterial tropism of Nipah and Hendra viruses. *Cell*. 2022;185:2523–2541.e30. doi: 10.1016/j.cell.2022.05.024
39. Pendeville H, Winandy M, Manfroid I, Nivelles O, Motte P, Pasque V, Peers B, Struman I, Martial JA, Voz ML. Zebrafish Sox7 and Sox18 function together to control arterial–venous identity. *Dev Biol*. 2008;317:405–416. doi: 10.1016/j.ydbio.2008.01.028
40. McCracken IR, Dobie R, Bennett M, Passi R, Beqqali A, Henderson NC, Mountford JC, Riley PR, Ponting CP, Smart N, et al. Mapping the developing human cardiac endothelium at single-cell resolution identifies MECOM as a regulator of arteriovenous gene expression. *Cardiovasc Res*. 2022;118:2960–2972. doi: 10.1093/cvr/cvac023
41. Kume T. Specification of arterial, venous, and lymphatic endothelial cells during embryonic development. *Histol Histopathol*. 2010;25:637–646. doi: 10.14670/HH-25.637
42. Herbert SP, Huisken J, Kim TN, Feldman ME, Houseman BT, Wang RA, Shokat KM, Stainier DYR. Arterial-venous segregation by selective cell sprouting: an alternative mode of blood vessel formation. *Science*. 2009;326:294–298. doi: 10.1126/science.1178577
43. Sacilotto N, Monteiro R, Fritzsche M, Becker PW, Sanchez-Del-Campo L, Liu K, Pinheiro P, Ratnayaka I, Davies B, Goding CR, et al. Analysis of Dll4 regulation reveals a combinatorial role for Sox and Notch in arterial development. *Proc Natl Acad Sci U S A*. 2013;110:11893–11898. doi: 10.1073/pnas.1300805110
44. McCracken IR, Baker AH, Smart N, De Val S. Transcriptional regulators of arterial and venous identity in the developing mammalian embryo. *Curr Opin Physiol*. 2023;35:100691. doi: 10.1016/j.cophys.2023.100691

45. Laurila PP, Soronen J, Kooijman S, Forsström S, Boon MR, Surakka I, Kaiharju E, Coomans CP, Van Den Berg SAA, Autio A, et al. USF1 deficiency activates brown adipose tissue and improves cardiometabolic health. *Sci Transl Med*. 2016;8:323ra–32313. doi: 10.1126/scitranslmed.aad0015
46. Wang Y, Nakayama M, Pitulescu ME, Schmidt TS, Bochenek ML, Sakakibara A, Adams S, Davy A, Deutsch U, Lüthi U, et al. Ephrin-B2 controls VEGF-induced angiogenesis and lymphangiogenesis. *Nature*. 2010;465:483–486. doi: 10.1038/nature09002
47. Madisen L, Zwingman TA, Sunkin SM, Oh SW, Zariwala HA, Gu H, Ng LL, Palmiter RD, Hawrylycz MJ, Jones AR, et al. A robust and high-throughput Cre reporting and characterization system for the whole mouse brain. *Nat Neurosci*. 2010;13:133–140. doi: 10.1038/nn.2467
48. Muzumdar MD, Tasic B, Miyamichi K, Li L, Luo L. A global double-fluorescent Cre reporter mouse. *Genesis*. 2007;45:593–605. doi: 10.1002/dvg.20335
49. Zhou P, Zhang Y, Ma Q, Gu F, Day DS, He A, Zhou B, Li J, Stevens SM, Romo D, et al. Interrogating translational efficiency and lineage-specific transcriptomes using ribosome affinity purification. *Proc Natl Acad Sci U S A*. 2013;110:15395–15400. doi: 10.1073/pnas.1304124110
50. Stuart T, Butler A, Hoffman P, Hafemeister C, Papalexi E, Mauck WM 3rd, Hao Y, Stoeckius M, Smibert P, Satija R. Comprehensive integration of single-cell data. *Cell*. 2019;177:1888–1902.e21. doi: 10.1016/j.cell.2019.05.031
51. Wickham H. Data analysis. In: Wickham H, ed. *ggplot2: Elegant Graphics for Data Analysis*. Springer International Publishing; 2016:189–201.
52. Bergen V, Lange M, Peidli S, Wolf FA, Theis FJ. Generalizing RNA velocity to transient cell states through dynamical modeling. *Nat Biotechnol*. 2020;38:1408–1414. doi: 10.1038/s41587-020-0591-3
53. Ishibashi A, Saga K, Hisatomi Y, Li Y, Kaneda Y, Nimura K. A simple method using CRISPR-Cas9 to knock-out genes in murine cancerous cell lines. *Sci Rep*. 2020;10:22345. doi: 10.1038/s41598-020-79303-0
54. Stringer C, Wang T, Michaelos M, Pachitariu MC. Cellpose: a generalist algorithm for cellular segmentation. *Nat Methods*. 2021;18:100–106. doi: 10.1038/s41592-020-01018-x
55. Wolf FA, Angerer P, Theis FJ. SCANPY: large-scale single-cell gene expression data analysis. *Genome Biol*. 2018;19:15. doi: 10.1186/s13059-017-1382-0
56. Palla G, Spitzer H, Klein M, Fischer D, Schaar AC, Kuemmerle LB, Rybakov S, Ibarra IL, Holmberg O, Virshup I, et al. Squidpy: a scalable framework for spatial omics analysis. *Nat Methods*. 2022;19:171–178. doi: 10.1038/s41592-021-01358-2